International Conference on Reactor Physics, Nuclear Power: A Sustainable Resource
Casino-Kursaal Conference Center, Interlaken, Switzerland, September 14-19, 2008

Refinement of the Santamarina-Hfaiedh energy mesh between 22.5 eV and 11.4 keV

A. Hébert[a*] and A. Santamarina[b]

[a]*École Polytechnique de Montréal, Montréal, Québec, CANADA H3C 3A7*
[b]*CEA Cadarache, DEN/DER/SPRC, Building 230, 13108 Saint Paul-lez-Durance, France*

Abstract

We are investigating the possibility to improve the accuracy of lattice calculations at neutron energies where resonance self-shielding effects are important. The proposed improvement are related to a refinement of the Santamarina-Hfaiedh energy mesh (SHEM) between 22.5 eV and 11.14 keV, increasing the total number of energy groups from 281 to 361 groups. The self-shielded multigroup cross sections are obtained using a simplified and straightforward subgroup model, used in association with the 361–group SHEM. Using as many energy groups permits to avoid the explicit representation of correlated slowing-down effects. The resulting equations are becoming sufficiently simple to reintroduce an accurate representation of other physical effects that are generally neglected, namely the mutual shielding effect between different isotopes and the temperature correlation effect caused by an explicit temperature gradient in a resonant isotope. Therefore, the longstanding problems of resonance escape factor underestimation and Doppler coefficient are solved using the SPM subgroup method on the SHEM–361 mesh. The resulting self-shielding model is shown to reach level of accuracies that are similar to those of a Monte-Carlo method.

1. Introduction

The advent of advanced reactor designs and the availability of better computing resources are the main motivations for the development of more accurate lattice code algorithms. The self-shielding model is a good candidate for accuracy improvements. We are proposing the development of a new self-shielding method consistent with the introduction of a finer energy mesh, using as many as 361 energy groups. The proposed self-shielding method is based on a simplification of the Ribon extended model[1],with the introduction of the capability to represent a temperature gradient in fuel. All the probability tables and weight correlated matrices are obtained with the CALENDF formalism.[4] The resulting formalism is referred as the subgroup projection method (SPM).[6]

The selected energy mesh, identified as

*Corresponding author, alain.hebert@polymtl.ca Tel: 1 (514) 340-4711 x. 4519

SHEM–361, is an adaptation of the 281–group Santamarina-Hfaiedh energy mesh (SHEM) introduced in Ref. 2. We have reworked the energy domain between 22.5 eV and 11.14 keV, increasing the number of groups from 38 to 118. Using more energy groups is required in order to avoid the use of the slowing-down correlation model, as introduced in the Ribon extended method. The remaining SHEM limits above 11.14 keV are left unchanged. A try-and-error approach was used to optimize the choice of the energy limits. The application of the SPM is limited to groups 56 to 173, as most correlation effects vanishes above 11.14 keV. Below 22.5 eV, the correlation effects are important, but are taken into account directly by the optimized fine mesh of the original SHEM structure.

Modern lattice designs involve the introduction of different fuel pins with various isotopic contents, with or without burnable poisons. In some cases, the burnable poison is mixed with depleted fuel, leading to lower temperature pins. It is not always possible to find a unique effective temperature for all occurrences of a given isotope in the lattice, so that the accurate representation of temperature gradient effects in fuel cannot be avoided.

2. The subgroup projection method

The basic idea behind the SPM approach is to simplify the Ribon extended approach by removing the slowing-down correlation model and by introducing a new cross section correlation model compatible with any solution approach of the neutron transport equation. The removing of the slowing-down correlation model is possible by using as many as 118 energy groups in the domain between 22.5 eV and 11.14 keV. The SPM, as described in Ref. 6, is available in release 4.0.2 of DRAGON.[9] Open-source cross section libraries in SHEM–361 Draglib format are also available.

The computing properties of the proposed SPM can be summarized as follows:

- The SPM is a subgroup approach based on CALENDF–type probability tables.[4]
- The self-shielding calculations are limited to energies above 22.5 eV. The SPM is used below 11.14 keV and the ST approach with physical probability tables is used above.
- The self-shielding calculations are kept apart from the main flux calculation, thank to the Livolant-Jeanpierre factorization presented in Ref. 1. We observed that fine-mesh moderator and coolant spatial discretization can be avoided, leading to important CPU cost savings for the self-shielding calculations. We currently recommend to define a simplified geometry for self-shielding, different from the more complex geometry used for the main flux calculation.
- The subgroup equations are leading to independent solutions of the neutron transport equations that can be solved in parallel on multiple CPUs.
- The new cross section correlation model can effectively represent both *mutual shielding effects* and *temperature gradient effects* in fuel, *without* introducing additional CPU costs other than those associated with the use of 118 groups.
- Using as many as 118 energy groups between 22.5 eV and 11.14 keV, the SPH treatment of the self-shielded cross sections is not required. However, the SPH treatment is kept in remaining groups with a lethargy width greater than 0.1.
- The SPM can represent isotopic correlation effects in three different ways. A non-correlation approximation is first available in case where resonances belonging to different isotopes are overlapping in a statistical way. A full-correlation model, similar to the model used in the ECCO lattice code, is available if different cross section sets are corresponding to the same isotope at different temperatures.[5] Finally, a general correlation model is available with the capability to represent any level of correlation, from no correlation to full correlation.

3. Numerical results

We have based our validation study on a subset made of eight Rowlands pin-cell benchmark cases[7] and two original test-cases featuring a temperature gradient in fuel. The comparisons

were made for light-water reactor pin-cells without leakage. Two types of pin-cell were studied, one UO2 fuelled (UOX), and the other UPuO2 fuelled, the latter in two versions with different isotopic compositions (MOX-1 and MOX-2). The effects of changes in temperature and water density were also calculated in order to examine the consistency of temperature calculation methods.

Five UOX cell cases were investigated. The first four are identical to those presented in Ref. 7. The fifth cell is an original PWR-HZP case, similar to case 3, with the arbitrary temperature profile of Table 1 in fuel. The goal if this test-case is to verify the numerical capabilities of the SPM to represent large temperature variations in a resonant isotope.

Table 1 Temperature gradient UOX rod.

Outer radius (cm)	Mixture	Temperature (K)
0.2529822	1	1200.
0.3346640	1	1000.
0.3577709	1	800.
0.3794733	1	700.
0.3898718	1	650.
0.4	1	600.
0.45	2	600.
0.6770275	3	573.6

The five MOX cell Benchmarks are also based on simple Wigner-Seitz unit cells. We investigated the effects of an increase in fuel temperature with two different isotopic vectors. Again, a fifth MOX cell was defined with the arbitrary temperature profile of Table 2 in fuel.

Table 2 Temperature gradient in MOX rod.

Outer radius (cm)	Mixture	Temperature (K)
0.259307	1	900.
0.343031	1	700.
0.366715	1	500.
0.388960	1	400.
0.3996186	1	350.
0.41	1	300.
0.475	2	300.
0.710879	3	293.6

The one-neutron source validation tests are limited to the resolved energy domain where it is possible to precisely define the resonant cross sections. The scattering kernel is assumed to be purely elastic. Cross sections were defined in the resolved energy domain and distributed over SHEM–361 energy groups 56 to 173, located between 22.5 eV and 11.14 keV. A 1.0 n/cm3/s source was placed in group number 56, located between 9.1188 keV and 11.138 keV and the absorption rates are computed in the remaining energy groups.

The UOX and MOX calculations use the same multigroup cross-section library based on the JEF 2.2 evaluation. Cross section libraries in PENDF and Draglib formats were build from scratch with NJOY release 99.259+upnea027. We selected the modified 361–group SHEM mesh presented in this study, with the correlation model set for all resonant isotopes. Draglib–formatted data is including temperature–dependent Autolib data for all resonant isotopes between 22.5 eV and 11.14 keV. The elementary lethargy width of the Autolib data is 5×10^{-4}.

Two computer codes have been used to perform these tests:

1. A computer code, named CESCOL, makes it possible to solve a fixed-source slowing-down equation using an elastic slowing-down operator for a mixture of heavy (resonant) isotopes in the resolved energy domain.[8] Heterogeneous cases can also be treated using collision probability (CP) techniques and used to generate reference solutions.

2. A self-shielding operator was written in the DRAGON Version4 lattice code[9] based on the SPM subgroup model. Self-shielded cross sections are obtained for a coarse energy grid and used in the existing CP flux solution operators. Consistency is emphasized by using the same CP calculation operator in both heterogeneous CESCOL and lattice code calculations.

We studied the absorption rates for the resonant isotopes in energy groups 56 to 173 and reported the discrepancies between CESCOL and lattice code calculations for every UOX benchmark.

The main purpose of the numerical tests was to compare the proposed self-shielding methodology with reference CESCOL calculations. The corresponding numerical results are presented in Tables 3 and 4 for various benchmark conditions.

We are reporting global error values for maximum $\epsilon^{\max}$, averaged $\bar{\epsilon}$ and integrated error ϵ^{int} isotopic and spatially-dependent ϵ^{int} values. The percent errors on absorption rates are plotted in Figs. 1 and 2. Note that the presence of the 1.0 n/cm^3/s source produces unphysical transients on absorption rates in groups 56 and 57.

An important observation is related to the use of the SPM–type general correlation model. In UOX cases, this model can be avoided in all cases, provided that the temperature gradients are treated with the ECCO–type full-correlation model. Neglecting the temperature correlation effects in the fifth test-case leads to a maximum error $\epsilon^{\max}$ reaching 84% in this case. In MOX cases, the correlation effects are more important. The application of the SPM–type general correlation model permits to reduce the maximum error below 4% and to divide by a factor of two the maximum error in each of the five MOX test-cases. It is important to note that the correlation model introduces no additional CPU costs, so that it can be left active in all situations. Both ECCO– and SPM–type correlation models permit to treat correctly the fuel temperature coefficient in presence of temperature gradient.

Table 3
Summary of UOX one-neutron source benchmarks. General correlation model is active.

	Case 1 Isothermal 293K	Case 2 Reduced H_2O density	Case 3 Fuel at 900K	Case 4 Isothermal 574K	Case 5 Temperature gradient in fuel
ϵ^{int} (%)	-0.059	-0.145	0.057	-0.014	0.070
$\bar{\epsilon}$ (%)	0.546	0.555	0.519	0.542	0.529
$\epsilon^{\max}$ (%)	3.337	2.781	2.513	2.602	2.419
in group	142	142	106	106	79
^{235}U ϵ^{int} (%)	0.353	0.361	0.360	0.351	0.362
^{238}U ϵ^{int} (%)	-0.242	-0.377	-0.066	-0.170	-0.048
^{238}U ϵ^{int} (%)					
shell 1	0.051	-0.117	0.357	0.201	0.520
shell 2	0.023	-0.144	0.353	0.218	0.419
shell 3	-0.299	-0.425	0.090	-0.085	-0.090
shell 4	-0.508	-0.611	-0.378	-0.515	-0.645
shell 5	-0.806	-0.884	-1.129	-1.095	-1.347
shell 6	-1.158	-1.262	-1.669	-1.540	-1.919

Table 4
Summary of MOX one-neutron source benchmarks. General correlation model is active.

	MOX fuel 1 Isothermal 300K	MOX fuel 1 Fuel at 560K	MOX fuel 2 Isothermal 300K	MOX fuel 2 Fuel at 560K	MOX fuel 1 Temperature gradient in fuel
ϵ^{int} (%)	0.098	0.157	0.140	0.211	0.211
$\bar{\epsilon}$ (%)	0.751	0.777	0.816	0.841	0.770
$\epsilon^{\max}$ (%)	3.079	3.458	3.495	3.508	3.318
in group	124	124	67	124	124
^{235}U ϵ^{int} (%)	0.420	0.402	0.403	0.382	0.389
^{238}U ϵ^{int} (%)	-0.209	-0.024	-0.204	-0.013	0.121
^{238}Pu ϵ^{int} (%)	0.237	0.303	0.355	0.421	0.343
^{239}Pu ϵ^{int} (%)	0.241	0.220	0.380	0.372	0.198
^{240}Pu ϵ^{int} (%)	0.597	0.536	0.504	0.465	0.569
^{241}Pu ϵ^{int} (%)	0.372	0.363	0.345	0.336	0.351
^{242}Pu ϵ^{int} (%)	0.657	0.400	0.464	0.278	0.206
^{241}Am ϵ^{int} (%)	0.342	0.335	0.324	0.313	0.317
^{238}U ϵ^{int} (%)					
shell 1	0.242	0.557	0.248	0.564	0.860
shell 2	0.079	0.401	0.089	0.410	0.530
shell 3	-0.309	-0.051	-0.301	-0.036	-0.350
shell 4	-0.570	-0.548	-0.571	-0.531	-0.743
shell 5	-0.946	-1.160	-0.946	-1.147	-0.770
shell 6	-1.513	-1.696	-1.513	-1.685	-1.853

Conclusions

The 361–group refined Santamarina-Hfaiedh energy mesh is permitting a better representation of self-shielding phenomena between 22.5 eV and 11.14 keV. The subgroup projection method is a good candidate for performing resonance self-shielding calculations in association with the refined energy mesh. It involves twice more energy groups than XMAS–172g mesh used in thermal reactors, but it allows high levels of accuracy. Furthermore, this optimized SHEM–361g could be used in FBR calculations in order to reduce drastically the computing time linked to the current 1968 group structure. The subgroup projection method is compatible with any type of solution of the transport equation. It permits the representation of distributed self-shielding effects, mutual shielding effects and temperature gradient effects. Particularly, it solves the long-standing problems of resonance escape factor and Doppler coefficient calculations in MOX assemblies and HCLWR lattices.

REFERENCES

1. Hébert, A., "The Ribon Extended Self-Shielding Model", *Nucl. Sci. Eng.*, **151**, 1–24 (2005).

2. Hfaiedh, N. and Santamarina, A., "Determination of the Optimized SHEM Mesh for Neutron Transport Calculations," *Proc. Top. Mtg. in Mathematics & Computations, Supercomputing, Reactor Physics and Nuclear and Biological Applications*, September 12 – 15, Avignon, France, 2005.

3. Hfaiedh, N., "Nouvelle Méthodologie de Calcul de l'Absorption Résonnante," Ph. D. thesis presented at Université Louis Pasteur Strasbourg, France, September 21, 2006.

4. Hébert, A. and Coste, M., "Computing Moment-Based Probability Tables for Self-Shielding Calculations in Lattice Codes", *Nucl. Sci. Eng.*, **142**, 245–257 (2002).

5. Grimstone M. J., Tulett J. D., and Rimpault, G., "Accurate Treatments of Fast Reactor Fuel Assembly Heterogeneity with the ECCO Cell

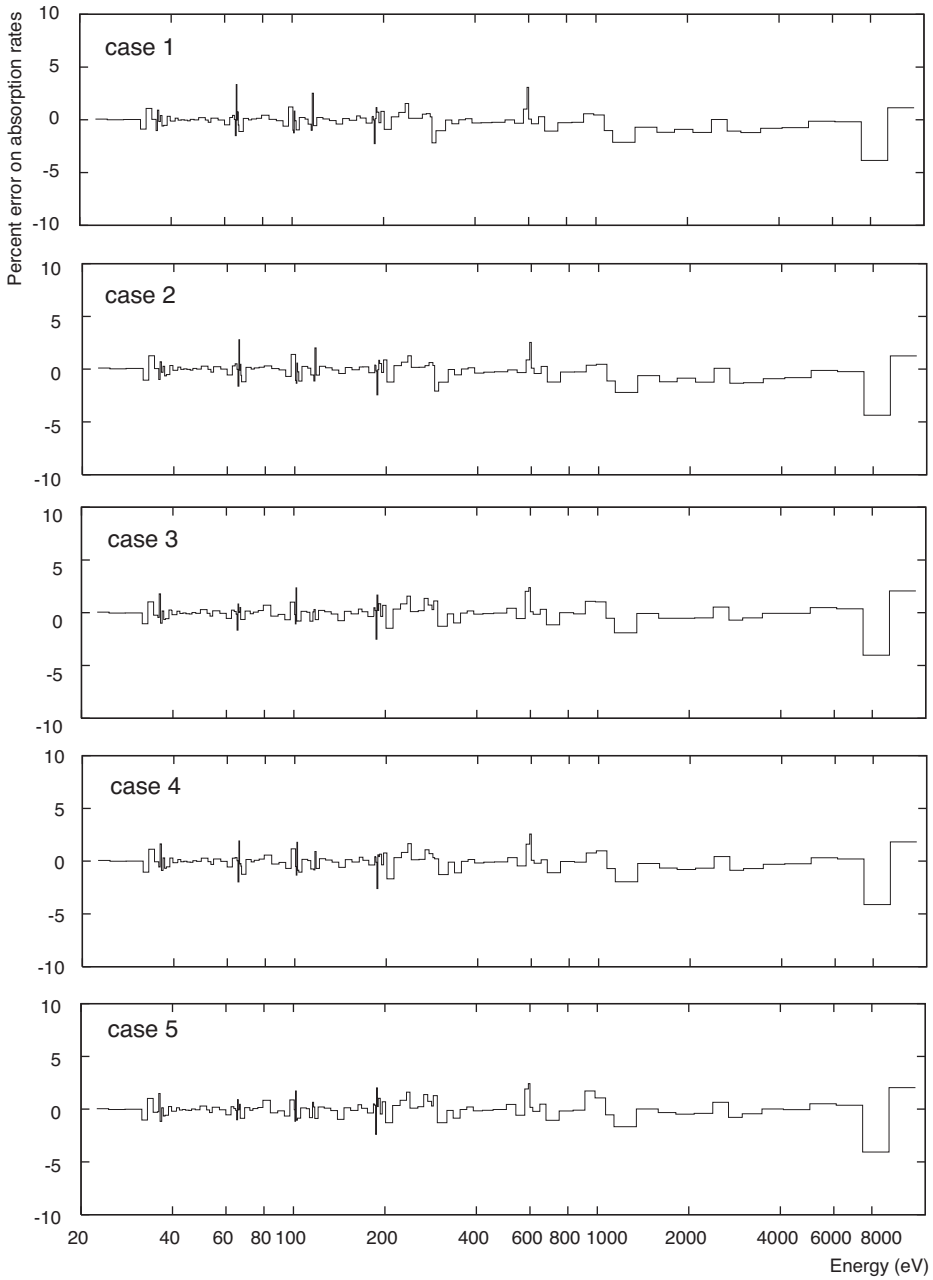

Fig. 1 Percent error on absorption rates. UOX cases. General correlation model is active.

Code", *Proc. Int. Conf. on the Physics of Reactors: Operation, Design and Computation – PHYSOR 90*, Marseille, France, p. IX:24, April 23-27 (1990).

6. Hébert, A., "Development of the subgroup projection method for resonance self-shielding calculations", Submitted for publication in *Nucl. Sci. Eng.*, (2008).

7. Rowlands, J. et al, "LWR Pin Cell Benchmark Intercomparisons. An Intercomparison study organized by the JEF Project, with contributions by Britain, France, Germany, The Netherlands, Slovenia and the USA.," *JEF Report to be published* , OECD/NEA Data Bank (1999).

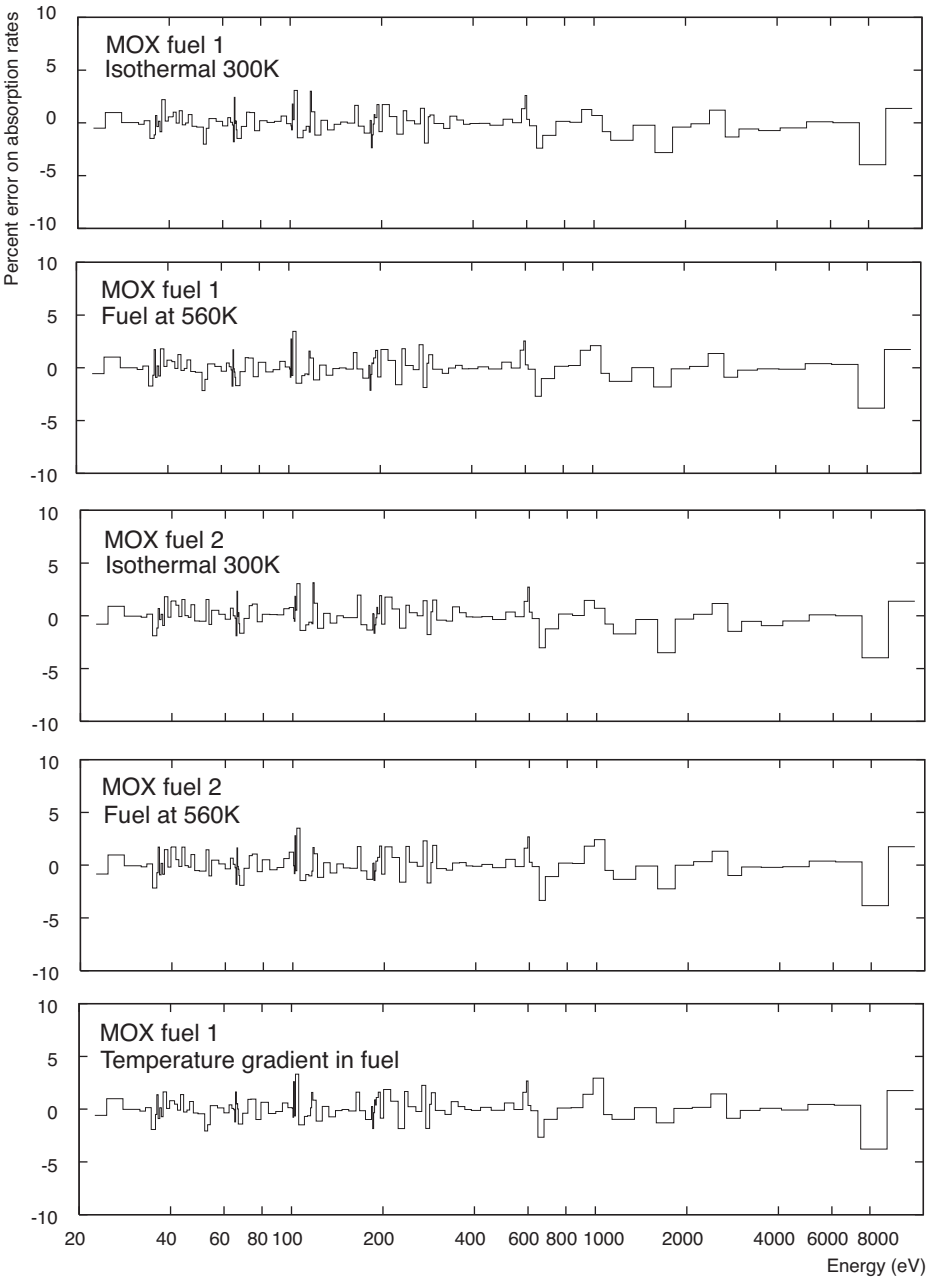

Fig. 2 Percent error on absorption rates. MOX cases. General correlation model is active.

8. Hébert, A. and Marleau, G., "Generalization of the Stamm'ler Method for the Self-Shielding of Resonant Isotopes in Arbitrary Geometries," *Nucl. Sci. Eng.*, **108**, 230 (1991).

9. Marleau, G., Hébert, A. and Roy, R., "New Computational Methods Used in the Lattice Code Dragon," *Proc. Int. Top. Mtg. on Advances in Reactor Physics*, Charleston, USA, March 8-11, 1992. Dragon Version4 and cross-section libraries can be downloaded from the web site at `http://www.polymtl.ca/merlin/`.

A The 361–group Santamarina-Hfaiedh mesh

The 361–group Santamarina-Hfaiedh mesh (SHEM–361) is based on the original SHEM–281 structure presented in Refs. 2 and 3. We have reworked the energy limits between 22.5 eV and 11.14 keV, increasing the number of groups in this domain from 38 to 118. The SPM is applied in groups 56 to 173 (included), corresponding to the resolved resonant energy groups. The improved structure of the SHEM–361 mesh is given in the following tables.

g	$U_{\min}$	$E_{\max}$ (eV)	Δu	
56	6.800	1.1138E+04	0.200	
57	7.000	9.1188E+03	0.200	
58	7.200	7.4658E+03	0.200	
59	7.400	6.1125E+03	0.200	
60	7.600	5.0045E+03	0.200	
61	7.800	4.0973E+03	0.163	
62	7.963	3.4811E+03	0.150	
63	8.113	2.9962E+03	0.104	
64	8.217	2.7002E+03	0.119	Na23 (2.85 keV), Mn55 (2.33 keV)
65	8.336	2.3973E+03	0.140	
66	8.476	2.0841E+03	0.140	
67	8.616	1.8118E+03	0.133	
68	8.749	1.5862E+03	0.166	
69	8.915	1.3436E+03	0.169	
70	9.084	1.1347E+03	0.064	U238 (1.14 keV)
71	9.148	1.0643E+03	0.080	U238 (991.8 eV)
72	9.228	9.8249E+02	0.077	U238 (958.8 eV, 937.3 eV)
73	9.305	9.0968E+02	0.089	
74	9.394	8.3222E+02	0.106	
75	9.500	7.4852E+02	0.100	
76	9.600	6.7729E+02	0.046	Pu240 (665.0 eV), U238 (661.3 eV)
77	9.646	6.4684E+02	0.054	
78	9.700	6.1283E+02	0.021	
79	9.721	6.0010E+02	0.012	Pu240 (596.8 eV), U238 (595.0 eV)
80	9.733	5.9294E+02	0.027	
81	9.760	5.7715E+02	0.068	
82	9.828	5.3920E+02	0.072	
83	9.900	5.0175E+02	0.100	
84	10.000	4.5400E+02	0.080	
85	10.080	4.1909E+02	0.070	Pu240 (405.0 eV)
86	10.150	3.9076E+02	0.050	
87	10.200	3.7170E+02	0.050	
88	10.250	3.5357E+02	0.053	U238 (347.8 eV)
89	10.303	3.3532E+02	0.047	
90	10.350	3.1993E+02	0.078	
91	10.428	2.9592E+02	0.026	U238 (291.0 eV), Zr91 (292.4 eV)
92	10.454	2.8833E+02	0.012	Pu240 (287.1 eV)

Mn55 (1.10 keV)

Mn55 (337 eV)

93	10.466	2.8489E+02	0.030	
94	10.496	2.7647E+02	0.030	
95	10.526	2.6830E+02	0.044	
96	10.570	2.5675E+02	0.060	
97	10.630	2.4180E+02	0.026	← Pu240 (239.3 eV), U238 (237.4 eV)
98	10.656	2.3559E+02	0.049	
99	10.705	2.2432E+02	0.056	
100	10.761	2.1211E+02	0.054	
101	10.815	2.0096E+02	0.025	
102	10.840	1.9600E+02	0.015	
103	10.855	1.9308E+02	0.015	
104	10.870	1.9020E+02	0.007	← U238 (189.7 eV)
105	10.877	1.8888E+02	0.007	
106	10.884	1.8756E+02	0.007	
107	10.891	1.8625E+02	0.007	← Pu240 (185.8 eV)
108	10.898	1.8495E+02	0.009	
109	10.907	1.8329E+02	0.045	
110	10.952	1.7523E+02	0.045	← Pu240 (170.1 eV)
111	10.997	1.6752E+02	0.027	← U238 (165.3 eV)
112	11.024	1.6306E+02	0.056	← Pu240 (162.7 eV)
113	11.080	1.5418E+02	0.050	← Pu240 (151.9 eV)
114	11.130	1.4666E+02	0.050	
115	11.180	1.3950E+02	0.050	← Pu240 (135.3 eV)
116	11.230	1.3270E+02	0.050	
117	11.280	1.2623E+02	0.046	← Pu240 (121.7 eV)
118	11.326	1.2055E+02	0.025	
119	11.351	1.1758E+02	0.009	← U238 (116.9 eV)
120	11.360	1.1652E+02	0.009	
121	11.369	1.1548E+02	0.023	
122	11.392	1.1285E+02	0.023	
123	11.415	1.1029E+02	0.043	
124	11.458	1.0565E+02	0.025	← Pu240 (105.1 eV)
125	11.483	1.0304E+02	0.009	← U238 (102.6 eV)
126	11.492	1.0211E+02	0.005	
127	11.497	1.0161E+02	0.005	
128	11.502	1.0110E+02	0.005	
129	11.507	1.0059E+02	0.033	
130	11.540	9.7329E+01	0.042	
131	11.582	9.3326E+01	0.050	← Pu240 (90.8 eV), Pu240 (92.5 eV)
132	11.632	8.8774E+01	0.056	
133	11.688	8.3939E+01	0.056	← U238 (80.7 eV)
134	11.744	7.9368E+01	0.039	
135	11.783	7.6332E+01	0.037	
136	11.820	7.3559E+01	0.023	← Pu240 (72.8 eV)
137	11.843	7.1887E+01	0.040	

138	11.883	6.9068E+01	0.033	
139	11.916	6.6826E+01	0.005	← Pu240 (66.6 eV)
140	11.921	6.6493E+01	0.005	
141	11.926	6.6161E+01	0.005	← U238 (66.0 eV), Pu239 (65.9 eV)
142	11.931	6.5831E+01	0.005	
143	11.936	6.5503E+01	0.007	
144	11.943	6.5046E+01	0.007	
145	11.950	6.4592E+01	0.015	
146	11.965	6.3631E+01	0.021	
147	11.986	6.2308E+01	0.039	
148	12.025	5.9925E+01	0.049	
149	12.074	5.7059E+01	0.054	
150	12.128	5.4060E+01	0.020	← Pu242 (53.46 eV)
151	12.148	5.2990E+01	0.023	
152	12.171	5.1785E+01	0.050	
153	12.221	4.9259E+01	0.036	← Hf176 (48.3 eV), Hf177 (48.9 eV)
154	12.257	4.7517E+01	0.028	
155	12.285	4.6205E+01	0.020	
156	12.305	4.5290E+01	0.025	← Mo95 (44.9 eV)
157	12.330	4.4172E+01	0.024	
158	12.354	4.3125E+01	0.023	← Nd145 (42.5 eV)
159	12.377	4.2144E+01	0.022	← Pu240 (41.6 eV)
160	12.399	4.1227E+01	0.037	← Ag109 (40.1 eV)
161	12.436	3.9730E+01	0.024	← In115 (39.6 eV)
162	12.460	3.8787E+01	0.026	← Pu240 (38.3 eV)
163	12.486	3.7792E+01	0.013	
164	12.499	3.7304E+01	0.012	
165	12.511	3.6859E+01	0.012	← U238 (36.7 eV), Hf179 (36.6 eV)
166	12.523	3.6419E+01	0.010	← Hf177 (36.1 eV, 37.0 eV)
167	12.533	3.6057E+01	0.010	
168	12.543	3.5698E+01	0.033	
169	12.576	3.4539E+01	0.043	
170	12.619	3.3085E+01	0.043	
171	12.662	3.1693E+01	0.128	
172	12.790	2.7885E+01	0.123	
173	12.913	2.4658E+01	0.090	← U235 (23.42 eV)